atmosphere

MDPI

Article

Relations between High Anticyclonic Atmospheric Types and Summer Season Temperature in Bulgaria

Vulcho Pophristov [1,2], Nina Nikolova [1], Simeon Matev [1] and Martin Gera [3,*]

[1] Faculty of Geology and Geography, Sofia University "St. Kliment Ohridski", 1504 Sofia, Bulgaria; vulcho.pophristov@cawri.bas.bg (V.P.); nina@gea.uni-sofia.bg (N.N.); smatev@gea.uni-sofia.bg (S.M.)
[2] Climate, Atmosphere and Water Research Institute at Bulgarian Academy of Sciences (CAWRI–BAS), 1784 Sofia, Bulgaria
[3] Faculty of Mathematics, Physics, and Informatics, Comenius University, 842 48 Bratislava, Slovakia
* Correspondence: martin.gera@fmph.uniba.sk

Abstract: The atmospheric circulation, not only near the surface but also at high altitudes, is probably the main factor determining the weather and climate of a given area, along with its latitude, altitude, the shape of the relief of the area and its surroundings, and the proximity of water basins of different sizes. The main objective of this study is to investigate the relationship between anticyclonic circulation types in the middle troposphere at the 500 hPa level and the seasonal summer temperature over the region of the central Balkan Peninsula, particularly Bulgaria. A previously compiled classification of atmospheric circulation is used, and the frequencies of the circulation types are correlated with the mean seasonal (monthly) temperature, where the extreme seasons and months are defined as the 10th percentile for cold summer seasons and months and the 90th percentile for warm ones. A positive and statistically significant correlation was found for the anticyclones located southwest of Bulgaria and a negative one for those located southeast of it. A comparison between the last two 30-year climatological periods (1961–1990 and 1991–2020) was also made, and an irrefutable decrease in the number of cold summer seasons from 257 to just 17 was found in the last 30 years, respectively, as well as a rapid increase in the number of extreme warm summer seasons from 26 to 263, encompassing all 15 meteorological stations studied.

Keywords: atmospheric circulation classification; circulation types at the 500 hPa level; extreme seasonal temperature; summer season; climate change

check for updates

Citation: Pophristov, V.; Nikolova, N.; Matev, S.; Gera, M. Relations between High Anticyclonic Atmospheric Types and Summer Season Temperature in Bulgaria. *Atmosphere* **2024**, *15*, 620. https://doi.org/10.3390/atmos15060620

Academic Editor: Alexander V. Chernokulsky

Received: 15 March 2024
Revised: 15 May 2024
Accepted: 16 May 2024
Published: 21 May 2024

Copyright: © 2024 by the authors. Licensee MDPI, Basel, Switzerland. This article is an open access article distributed under the terms and conditions of the Creative Commons Attribution (CC BY) license (https://creativecommons.org/licenses/by/4.0/).

1. Introduction

One of the main goals of synoptic climatology is not just to classify atmospheric circulation types according to certain rules assessing baric fields but also to compare the frequencies of the types with a great variety of meteorological elements and to study the dependencies between atmospheric circulation patterns and meteorological phenomena. Numerous studies have been dedicated to investigating extreme events during specific synoptic conditions and their trends over recent decades, which is an important task, especially in the context of climate change. For example, hot spells or heat waves and their relationship with atmospheric circulation are explored in [1–4] for different regions of Europe and in [5–10] for other parts of the world. Synoptic analyses of cold spells have been performed for many regions and focus either on climatological aspects [11–13] or on concrete extreme cold periods [14–16]. Cases of extreme precipitation with the potential to cause flood hazards and other dangerous events such as landslides are also depicted in a lot of research [17–25]. There are several approaches to composing circulation types in atmospheric circulation classifications. Some of them use the direction of the air masses near the land surface as a main variable for naming and numbering the baric formations of circulation types, such as the classification by Lamb [26,27] for the British Isles.

The other main approach to determining circulation types is to use the position of the centre of the baric formation (cyclone/anticyclone) towards the territory of interest. Such classifications include the widely known "Grosswetterlagen", composed by Hess and Brezowsky for the central parts of Europe [28–30], Maheras's classification composed for Greece [31–33], and the classification for Bulgaria [34–36], used in the present work and explained in detail in [34]. The latter classification is made for both SLP (sea level pressure) and 500 hPa geopotential height at approximately 5.5 km above sea level in the middle troposphere. A great dependence on the atmospheric circulation between both baric levels occurs. In the front part of the high trough, an airflow divergence of 500 hPa exists, which causes a decrease in the air pressure at that level. Meanwhile, this is a reason for upward movements between the surface level and the 500 hPa level, i.e., the convergence of the airflow near the surface and, respectively, the cyclonic circulation there. The opposite processes are valid in the back parts of the high trough, where a convergence of the airflow exists, followed by downward movements, as the result is anticyclonic circulation near the surface, below this part of the high trough. This is one of the reasons why research dedicated to atmospheric circulation classifications at 500 hPa makes sense.

In the northern hemisphere, the airflow at the front of the high trough at 500 hPa comes from the southern quarter, bringing warmer air masses to the investigated area. For the Balkans, these air masses originate from the Mediterranean or North Africa. In the back parts of the high trough, the winds are from the northern quarter and cause cold penetration in the middle troposphere. Many studies investigate the dependencies between the circulation at 500 hPa and various meteorological manifestations. The connection between synoptic types at 500 hPa and fires has been examined for Canada [37,38], Alaska [39], the western Mediterranean region [40,41], and Australia [42]. In the field of air quality, atmospheric and synoptic conditions are examined for continuous and severe weather pollution in many regions like China [43–48], other parts of Asia [49,50], the Arctic [51], and the Iberian Peninsula [52]. Other articles assess the influence of circulation at 500 hPa on climatological seasons [53,54] or concentrate on specific cases or consequences of some meteorological phenomenon [55,56].

Considering temperature as a meteorological element, studies mostly concentrate on their minimum or maximum values and, to a lesser extent, on their average values. This is associated with the fact that the minimum and maximum temperatures are extreme values, which are of interest if the purpose of the study is to investigate extreme meteorological phenomena. The average daily or monthly temperatures could also be used to explore extreme events because the minimums and maximums might be considered as a function of the average values, but the choice depends on every concrete research goal. Regardless of which temperature parameter is chosen, a predefined rule is required to define an extreme temperature event. One of the solutions is to choose a constant number as a threshold, but the problem with using this approach is that it is defined for a particular geographic region, as the value varies and is dependent on latitude and climate characteristics, altitude, and the season of the year [57,58]. This is the main reason why relative thresholds of the empirical distribution of the temperature, or so-called percentiles, take part and are widely used. This method allows for comparing data gathered from meteorological stations in different geographical areas and with different climates and was proposed in [59,60]. Therefore, it is ensured that a given part of the temperature observations are extreme by definition, regardless of their range or impact. [61,62]. Temperature extremes are most often determined using percentiles ranging from the 1st to the 10th for cold days and from the 90th to the 99th for warm or hot days and are presented and commonly used in various climatological indices [63–65]. Percentile indices could be defined for different time frames. For example, [66,67] calculates the percentile for the entire calendar year, for the entire summer season (June, July, August) [68], and separately for every summer month [69].

The main goal of the current work is to investigate the relation between the anticyclonic circulation types at 500 hPa, formed according to the rules in [34], and summer seasonal temperature, respectively, for every summer month in the period 1961–2020,

which includes the last two climatological periods 1961–1990 and 1991–2020. A comparison between extremely warm and cold seasons for these two periods is also performed. The thresholds of the 10th and 90th percentiles of the examined 60-year period are used for determining the extreme cold and warm temperature months and seasons. This approach is applied not only to the temperature time series but also to the frequencies of the circulation types. Conclusions are drawn for each type based on its correlation with seasonal and monthly temperatures.

2. Materials and Methods

The studied area includes climatological data from 15 meteorological stations (Table 1 and Figure 1), which are relatively evenly distributed and situated in different climate zones. Thirteen of them are within the territory of Bulgaria, and two, Nis (Serbia) and Calaras (Romania), are situated near the Bulgarian border. The Musala and Murgash stations represent high mountain areas above 2000 m a.s.l. and mid-mountain areas between 1000 and 2000 m a.s.l. According to the Köppen classification [70], they have a typical mountain climate, corresponding to E and Dfc zones. The stations Sofia, Kjustendil, and Razgrad, at an altitude between 346 and 586 m a.s.l., correspond to the climate zone Cfb. It is characterized by a hot summer and cool winter with relatively evenly distributed annual precipitation. The southernmost stations in the studied area are Sandanski and Kardzhali, which fall into the Csa climate zone, characterized by hot and dry summers, mild winters, and maximum precipitation in the cold half of the year. The remaining stations are in the Cfa zone.

Table 1. Coordinates and altitude (m a.s.l.) of the meteorological stations used in the research and their climate zone according to Köppen climate classification.

Station	Altitude	Latitude	Longitude	Climate Zone
Vidin	31	43°59′39.1″ N	22°51′09.1″ E	Cfa
Pleven	160	43°24′26.5″ N	24°36′22.4″ E	Cfa
Razgrad	346	43°33′58.5″ N	26°30′27.7″ E	Cfb
Calarasi	20	44°12′21.0″ N	27°20′18.0″ E	Cfa
Varna	39	43°12′45.0″ N	27°57′08.3″ E	Cfa
Burgas	21	42°29′51.7″ N	27°28′57.7″ E	Cfa
Sliven	259	42°40′39.9″ N	26°20′23.5″ E	Cfa
Kardzhali	337	41°38′48.2″ N	25°23′07.2″ E	Csa
Plovdiv	154	42°08′03.5″ N	24°48′09.0″ E	Cfa
Sandanski	206	41°33′00.0″ N	23°16′02.5″ E	Csa
Kjustendil	520	42°17′01.7″ N	22°42′47.3″ E	Cfb
Musala	2925	42°10′45.6″ N	23°35′06.7″ E	E
Murgash	1687	42°49′58.4″ N	23°40′07.7″ E	Dfc
Sofia	586	42°39′13.2″ N	23°22′58.3″ E	Cfb
Nis	202	43°19′35.2″ N	21°53′51.4″ E	Cfa

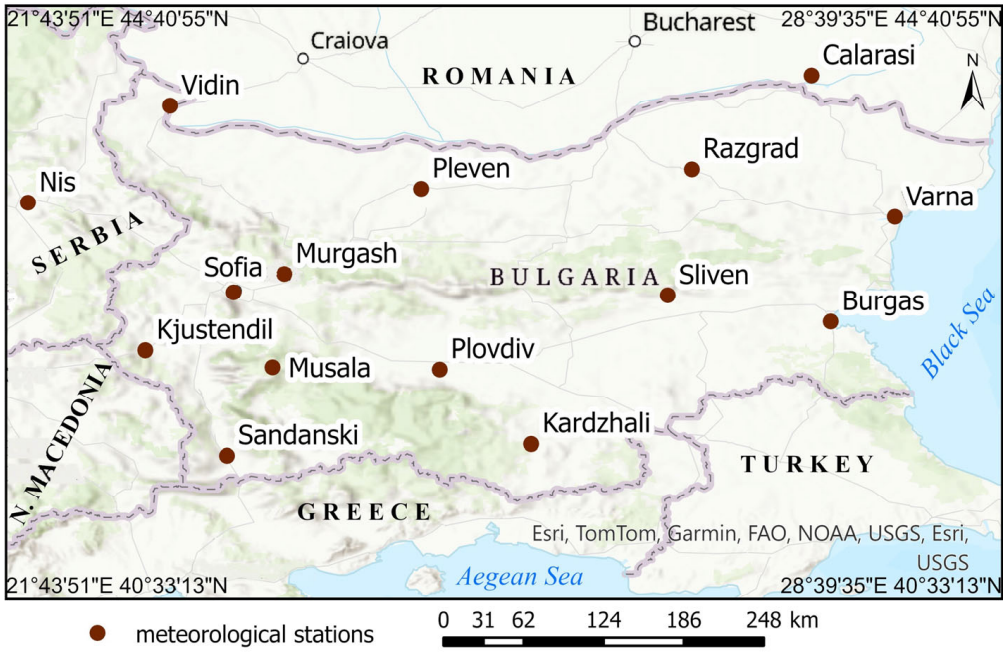

Figure 1. Geographical distribution of the meteorological stations. This territory represents the Southeast part of Europe.

The period of the study was 1961–2020, and the monthly and correspondingly summer seasonal temperature values were calculated according to the climatological methodology [71,72], based on the daily average values derived from three fixed-in-time daily observations at 7, 14, and 21 local standard time, as the evening observation was weighted twice (1).

$$T_{(ave)} = (T_7 + T_{14} + 2 \times T_{21})/4 \quad (1)$$

Summer temperatures were obtained by averaging the monthly values for June, July, and August.

The atmospheric circulation classification used in the study was carried out using a subjective (manual) approach to the circulation types. This means that every day in the examined period was classified manually, according to some predefined rules, without using an automatic execution of a numerical algorithm. The classification was based on the data and isolines for a geopotential height at 500 hPa, derived from 20th-century reanalyses, NCEP CFSR/GFS reanalyses, and NCEP/NCAR reanalyses [73–75]. The visualisations from wetter3.de were mainly used for this purpose, where the data for these three reanalyses were united, covering different periods [76]. We considered the atmospheric circulation to be of an anticyclonic type in cases where a certain anticyclone covers the territory of Bulgaria, regardless of where its centre is located. According to the position of the centre of the anticyclone relative to the territory of Bulgaria, five types of anticyclonic circulation at 500 hPa were determined. The centre of anticyclone type A1 is situated northwest of Bulgaria, north of the 45th parallel, and west of the 25th meridian, and A2 is north of the 40th parallel and east of the 25th meridian. Type A3 is over the country between the 40th and 45th parallel and the 20th and 30th meridian. The anticyclonic type A4 is often a ridge from the Azores High, considered as such if its centre is west of the 20th meridian and south of the 45th parallel. The centre of type A5 is east of the 20th meridian and south of the 40th parallel (Figure 2).

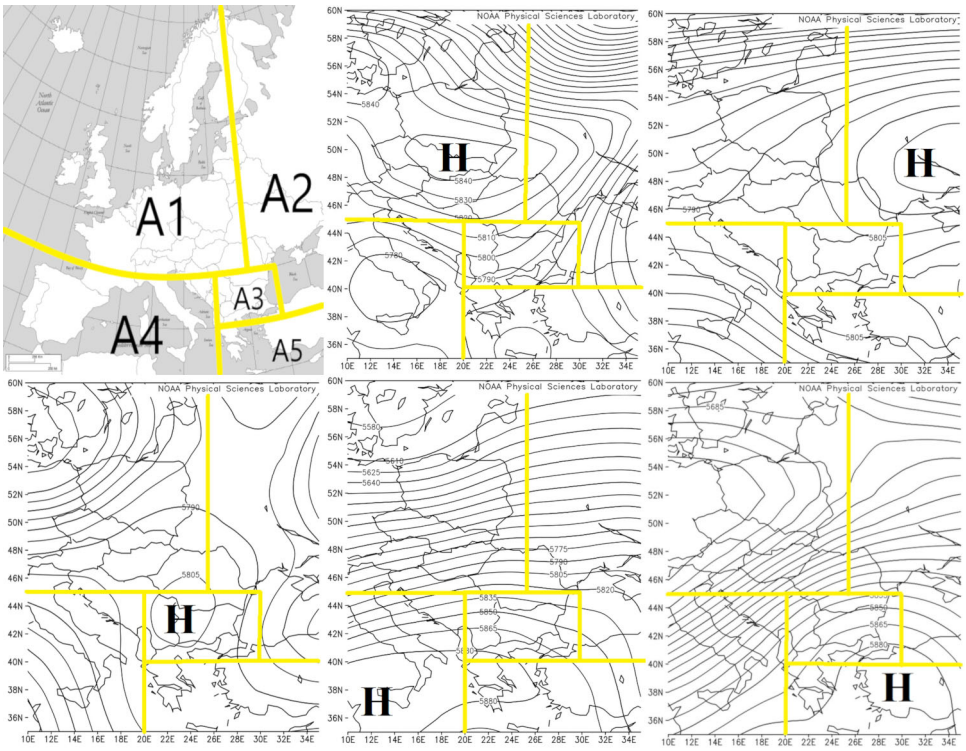

Figure 2. The visualizations of anticyclonic types at 500 hPa are acquired from the NOAA Physical Sciences Laboratory (PSL). **First row** (**left**)—a scheme showing the position of the centre of every circulation type (source: basemap of Europe from https://alabamamaps.ua.edu, accessed on 15 May 2024). **First row** (**middle**)—A1; **First row** (**right**)—A2; **Second row** (**left**)—A3; **Second row** (**middle**)—A4; **Second row** (**right**)—A5. Black curves illustrate isolines of geopotential height at the 500 hPa level. Yellow lines represent borders between the anticyclonic types. Source: NOAA-CIRES 20th Century Reanalysis (V2c).

The summer (June, July, August) frequencies of the anticyclonic types at 500 hPa over the 60 years (1961–2020) are presented in Table 2. The second column represents the frequencies concerning all circulation types (anticyclonic and cyclonic) at that baric level, while the third column shows the frequencies only amongst anticyclonic types.

Table 2. Summer frequencies (1961–2020) of the anticyclonic (AC) circulation types at the 500 hPa level in %.

Type	% of All Types	% of AC Types
A1	1.6	4.0
A2	0.8	2.0
A3	1.3	3.3
A4	28.7	71.9
A5	7.5	18.8
All (AC)	39.9	100.0

Types A1, A2, and A3 have very low frequencies compared to the A4 and A5 types; hence, their climatological influence is relatively small, and that is why more attention is paid to the last two. The presence of the A1 type at the 500 hPa level leads to a northern direction of airflow at that baric level, and often, there is the presence of a high trough east of the anticyclone. In the presence of of A2, the wind direction at the 500 hPa level over Bulgaria comes from the eastern quarter, and it depends on the exact position of the isolines of the baric field. The A3 type's centre is over the territory of Bulgaria, so it is the reason for

there being almost no wind in this area (Figure 2). A4 has the highest frequency, not only among anticyclonic types but also among all circulation types at 500 hPa, during the summer season. It has a leading climate-forming role, especially in the summer. Its frequency is 28.7% for all types and 71.9% for the anticyclonic types. The A4 type causes westerly and south-westerly winds and thus causes relatively warmer air masses, predominantly from the Mediterranean or Northern Africa, to reach the middle levels of the troposphere above central parts of the Balkan peninsula and especially Bulgaria. The frequency of type A5 is second in value, although it is much smaller than that of A4. Depending on the exact position of the baric formation, the winds have a southwestern or southern direction. In almost all cases with A5, there is a trough situated west of it, over a territory most often above the middle of the Mediterranean. This fact means that over this region, relatively colder air masses are already intruding, through the counterclockwise directions of the airflow of the system of this high trough. As a consequence, this south–western direction of the winds in the neighbouring A5 anticyclone, in most cases, has, to some degree, a cooling effect in the middle troposphere over the territories of the Balkan peninsula, and because the circulation in the western back part of the high anticyclone is similar to that in the front part of the high trough and some kind of cyclonic circulation at lower atmospheric levels, respectively, cloudiness or even precipitation can occur.

The seasonal distribution of anticyclonic circulation types is shown in Figure 3. The domination of type A4 over A5 is so substantial only in the summer season. In the transitional seasons (spring and autumn), A4 still prevails, but in the winter, the frequency of A5 is even greater than that of A4. Only A4 and A3 have their maximums in the summer, A2 in the autumn, and A5 and A1 in the winter.

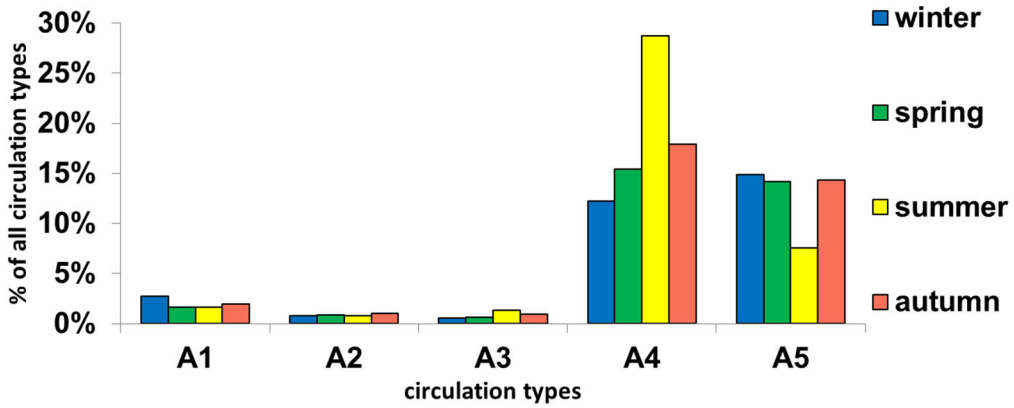

Figure 3. Seasonal distribution of the anticyclonic circulation types at 500 hPa as % of all circulation types for the period 1961–2020.

To find a relation between the frequencies of the circulation types and the summer seasonal temperature, Pearson's correlation coefficient was used, with a standard level of significance ($\alpha = 0.05$) determined by *t*-tests. According to the chosen significance level and the length of the row of 60 values concerning the period (1961–2020), the calculated statistically significant correlation coefficients have values greater than 0.26. For assessing the tendencies of the anticyclonic types at 500 hPa, the non-parametric Mann–Kendall test [77] and Sen's slope estimator [78] were applied. The calculations of correlations and trends on a monthly and seasonal basis were carried out through MS Excel's RealStatistics software ver.8.7 [79].

3. Results and Discussion

3.1. Extremely Warm and Cold Summer Seasons in 1961–1990 and 1991–2020

Extreme values of the seasonal and monthly temperatures in the present work are defined as less than or equal to the 10th percentile ($\leq$p10) for extremely cold and greater than or equal to the 90th percentile ($\geq$p90) for extremely warm months or seasons, concerning

the period 1961–2020. Table 3 shows the ratios between the last two 30-year climatological periods (1961–1990 and 1991–2020) of extremely cold and warm summer months, respectively, providing a summary for the season and separate values for the months June, July, and August, for each of the meteorological stations included in the research. Left of the slash are the values in the period 1961–1990 and, to the right of it, for 1991–2020. The number of extremely cold months decreased rapidly from 257 months in 1961–1990 to just 17 months in 1991–2020. This represents a fifteen-fold decrease. Conversely, the number of extremely warm months increased from 24 in 1961–1990 to 247 in 1991–2020, which is over ten times more. This increase in hot extremes was found by Malcheva et al. [80], who stated that in the Cfa and Csa climate zones of Southeastern Europe, the number of warm days in the period 1991–2020 was 12–13 higher than in 1961–1990. Zahradníček et al. [81] point out the increasing number of anticyclonic types as the cause of extremely hot events in the Czech Republic.

Table 3. The ratios between the last two climatological periods, **1961–1990/1991–2020**, of extremely cold **(p10)** and extremely warm **(p90)**, respectively, summer seasons and summer months.

Station	Summer		June		July		August	
	p10	**p90**	**p10**	**p90**	**p10**	**p90**	**p10**	**p90**
Vidin	20/0	2/17	7/0	0/7	7/0	2/4	6/0	0/6
Pleven	18/0	3/16	6/0	1/6	6/0	2/4	6/0	0/6
Razgrad	16/1	2/16	5/1	1/5	6/0	1/5	5/0	0/6
Calarasi	19/1	2/19	6/0	1/7	5/1	1/6	8/0	0/6
Varna	17/1	0/21	6/0	0/7	6/0	0/7	5/1	0/7
Burgas	18/0	0/21	6/0	0/6	6/0	0/7	6/0	0/8
Sliven	15/3	1/18	5/1	1/5	5/1	0/6	5/1	0/7
Kardzhali	14/4	2/16	4/2	1/5	5/1	1/5	5/1	0/6
Plovdiv	18/0	0/18	6/0	1/6	6/0	0/6	6/0	0/6
Sandanski	18/1	3/17	6/0	1/5	6/0	2/6	6/1	0/6
Kjustendil	16/2	2/18	5/1	0/6	6/0	2/5	5/1	0/7
Musala	17/1	3/16	6/0	0/6	6/0	2/5	5/1	1/5
Murgash	17/1	2/16	6/0	0/6	6/0	2/4	5/1	0/6
Sofia	18/0	2/17	6/0	0/7	6/0	2/4	6/0	0/6
Nis	16/2	2/17	6/0	0/6	6/0	2/5	4/2	0/6
ALL	257/17	26/263	86/5	7/90	88/3	19/79	83/9	1/94

Cases with extremely cold months in 1991–2020 and extremely warm months in 1961–1990 are small in number, so they could be mentioned just as exceptions in their relevant periods. For p10 in June, these are 1992 and 2005, registered only in three stations in southern Bulgaria—1992 in Kjustendil and Kardzhali and 2005 in Kardzhali and Sliven. The threshold of p90 was reached in several stations in southern Bulgaria in June 1981, while July 1987 was extremely warm in the western part of Bulgaria. August 1997 was extremely cold, falling into the range of p10.

3.2. Correlation between Summer Temperature and the Anticyclonic Types at 500 hPa

In this subsection are presented the calculated Pearson's correlation coefficients between summer seasonal temperature and the frequency of each anticyclonic type at the 500 hPa level for all 15 meteorological stations (Table 4). Type A1 has a negative and statistically significant correlation for all the stations, as it is stronger in the western parts of Bulgaria, so its cooling influence is a little more significant in the western parts of the country. The correlation of A2 with seasonal temperature is negative for most of the stations but statistically insignificant for all of them, and the values are close to zero. A3 also has

a slight and statistically insignificant correlation with the temperature for all the stations, but unlike A2, it is positive for almost all the stations. The frequencies and, respectively, their climatological influence on the regions of types A4 and A5 are much greater, and the spatial distribution of the correlation coefficients will be shown in more detail. The type with the greatest positive correlation with the summer seasonal temperature amongst all anticyclonic circulation types at 500 hPa is type A4. The correlation values are highest in western Bulgaria, decreasing slightly to the east. The lowest values are registered on the Black Sea seaside in Varna and Burgas, as Varna is the only station where the correlation coefficient is not statistically significant. This fact means that the Azores High's, at 500 hPa, influence on the temperature at the surface slightly weakens in the eastern direction because of the cooling effect of the Black Sea during the summer on one side, and also that the eastern parts of Bulgaria are always more or less on the periphery of the anticyclone concerning type A4. As seen from Table 4, A5 frequencies have negative correlations with summer seasonal temperature, and therefore this type has a relatively strong cooling effect for Bulgaria.

Table 4. Pearson's correlation coefficients between summer seasonal temperature, summer month (VI, VII, VIII) average temperature for the types A4 and A5, and the seasonal and monthly frequencies of anticyclonic types at the 500 hPa level concerning the meteorological stations used in the study. The values in italics are statistically significant at a significance level of 0.05. Bold monthly values mark the maximal correlation coefficient amongst the three summer months for the A4 and A5 types.

Station	A1	A2	A3	A4	VI	VII	VIII	A5	VI	VII	VIII
Vidin	*−0.57*	−0.20	0.12	*0.56*	*0.29*	*0.56*	***0.66***	*−0.50*	−0.17	***−0.42***	−0.25
Pleven	*−0.49*	−0.15	0.23	*0.59*	*0.29*	*0.66*	***0.68***	*−0.42*	−0.17	***−0.28***	−0.20
Razgrad	*−0.47*	−0.06	0.12	*0.54*	*0.33*	***0.61***	*0.60*	*−0.30*	−0.09	***−0.34***	−0.25
Calarasi	*−0.47*	−0.04	−0.06	*0.40*	0.19	*0.50*	*0.51*	*−0.44*	***−0.27***	−0.20	−0.13
Varna	*−0.37*	0.07	0.01	0.25	0.07	*0.31*	***0.39***	*−0.27*	−0.15	**−0.21**	−0.05
Burgas	*−0.42*	−0.01	0.03	*0.31*	0.15	*0.34*	***0.44***	*−0.38*	−0.20	**−0.25**	−0.14
Sliven	*−0.48*	−0.09	0.05	*0.47*	*0.28*	*0.51*	***0.53***	*−0.39*	−0.19	**−0.25**	−0.13
Kardzhali	*−0.43*	0.01	0.06	*0.48*	*0.32*	***0.60***	*0.54*	−0.13	0.01	**0.06**	−0.02
Plovdiv	*−0.55*	−0.16	0.10	*0.48*	*0.27*	*0.55*	***0.57***	*−0.51*	−0.21	***−0.32***	−0.25
Sandanski	*−0.58*	−0.10	0.18	*0.59*	*0.34*	***0.66***	*0.62*	*−0.42*	−0.09	**−0.24**	−0.16
Kjustendil	*−0.53*	−0.01	0.18	*0.56*	*0.32*	*0.63*	***0.64***	*−0.31*	−0.10	**−0.21**	−0.11
Musala	*−0.53*	−0.04	0.08	*0.53*	*0.31*	*0.65*	***0.65***	*−0.47*	−0.20	**−0.22**	−0.15
Murgash	*−0.56*	−0.10	0.12	*0.60*	*0.38*	*0.66*	***0.68***	*−0.44*	−0.19	***−0.29***	−0.18
Sofia	*−0.57*	−0.17	0.15	*0.54*	*0.29*	*0.58*	***0.66***	*−0.52*	−0.24	***−0.43***	−0.23
Nis	*−0.56*	−0.10	0.12	*0.56*	*0.31*	*0.55*	***0.69***	*−0.42*	−0.14	***−0.36***	−0.21

Table 4 presents the correlation coefficients of the summer months (June, July, and August) between temperatures and the frequencies of types A4 and A5, including the seasonal correlations for all anticyclonic types at 500 hPa. Bold monthly values mark the maximal correlation coefficient amongst the three summer months for A4 and A5. For twelve of the fifteen meteorological stations, the maximum is in August concerning A4, only Kardzhali and Sandanski in southern Bulgaria and Razgrad have a maximum in July. The maximum correlation coefficients for A5 are in July, and the only exception is Calarasi, with a maximum in June. Most of the monthly values of the correlation coefficients are not statistically significant in June and August for A5, while for July, the correlation coefficients are statistically significant for the stations in the northern part of Bulgaria. It is evident that the monthly correlation coefficients for type A5 are smaller than the seasonal ones. This fact is probably because the monthly data series of type A5's frequency has many zero values over the years. The spatial distributions of the Pearson's correlation coefficients between the frequency of types A4 and A5 and the summer seasonal temperature show

differences across the territory of the country in connection with the influence of orography and proximity to the Black Sea (Figures 4 and 5).

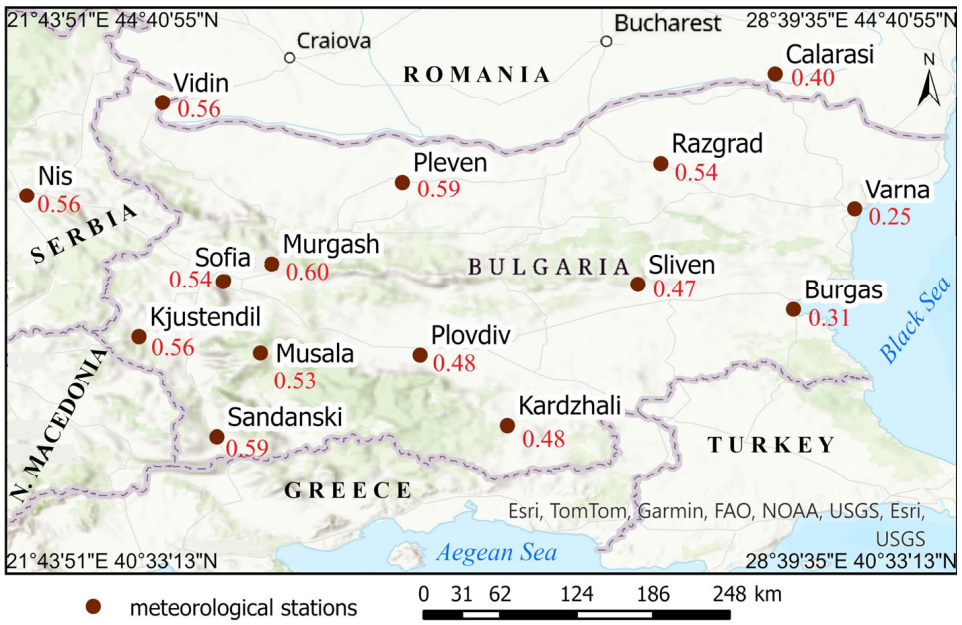

Figure 4. Spatial distribution of Pearson's correlation coefficients between frequency of A4 circulation type at the 500 hPa level and summer temperature (1961–2020).

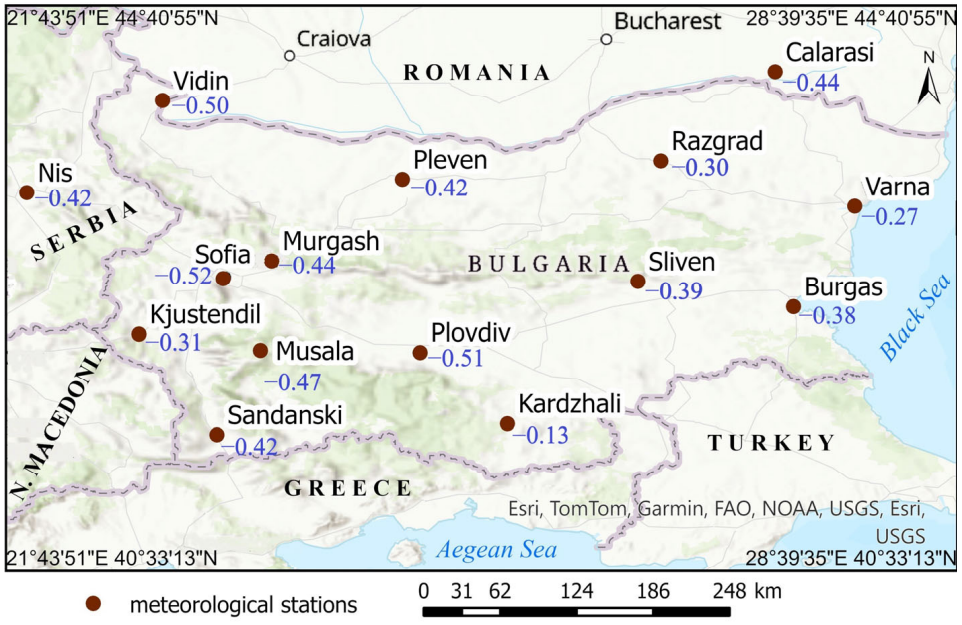

Figure 5. Spatial distribution of Pearson's correlation coefficients between frequency of A5 circulation type at the 500 hPa level and summer temperature (1961–2020).

The opposite correlations between the frequency of circulation types A4 and A5 and summer air temperatures are a result of the different synoptic situations during the two types of anticyclonic circulation. For example, in most cases, during A4, there is prevailing zonal circulation over the continent. Sfîcă et al. [82] pointed out that increasing diurnal temperature range and strong heating in summer are related to west anticyclonic circulation patterns. Type A5 is often an anticyclonic ridge from the south, and when it occurs west of it, there is a baric trough over the central Mediterranean. In such a situation, in summer,

relatively colder air exists in these regions, and this pattern affects the adjacent anticyclone, which causes negative correlation coefficients between the frequency of A5 at 500 hPa and temperature. In this case, more meridional than zonal circulation develops over the whole region of Europe, not only in Southeastern Europe. Bartoszek [83] found a higher-than-average frequency of anticyclonic and northerly circulation in summer over East–Central Europe.

3.3. Dependencies between Seasonal and Monthly Temperature and the Frequencies of the Anticyclonic Types at the 500 hPa Level

The distributions of the frequencies of circulation type A4 and the average temperature from all the studied meteorological stations are presented in Figure 6, where (a) is on a seasonal basis, (b), (c), and (d) are for the months June, July, and August. The blue dots represent the values in the years when both temperature and the frequencies of type A4 fall in the 10th percentile of the data series. Red dots represent the 90th percentile. On a seasonal basis (a), the tenth percentile requirement is fulfilled in the years 1976 and 1969, as 1976 is the coldest summer in the period (1961–2020). The warmest summers in that period were 2012 and 2007, and they are also the summer seasons with the highest frequencies of type A4. The coldest June (b) occurred in 1989, and this was also the only June with no registered days of A4 in the 60-year period studied. The other year in the 10th percentile for both temperature and the number of days with A4 is 1976, as June 2012, 2007, and 2003 were the warmest Junes, and 2012 and 2003 had the maximum number of days with A4 in June. The years 2012 and 2007 were the warmest for July (c), and 1987 fulfils the requirement too. The second coldest July was in 1971, with a minimum of just 1 day with A4, while the coldest was in 1969. The warmest August (d) was in 2010, but the 90th percentile was exceeded for both temperature and the frequency of A4 in 1992 and 2008. The coldest August was in 1976, when no days with A4 were recorded. The distribution of the dots reveals the positive correlation between the frequency of A4 and the temperature, as is visible to various degrees in all four graphs.

The same approach was used concerning type A5, and its distribution of frequencies and all the stations' average temperatures are shown in Figure 7. As opposed to type A4, A5 has a negative correlation with the temperature, although the correlation coefficients every month show that most of them are not statistically significant (Table 4). The negative correlation in this case means that the values below the 10th percentile of one parameter are compared to those above the 90th percentile of the other parameter. For example, the high temperatures over the 90th percentile are associated with a low number of days with type A5, and vice versa! On a seasonal basis (Figure 7a), the negative correlation is well visible, as the highest values of the temperature in 2012, 2003, and 2019 are correlated with a low number of days of type A5 below the 10th percentile. The summer of the year 1969 fulfilled the opposite requirements for the temperature to be equal to or below the 10th percentile and the number of days with A5 equal to or above the 90th percentile, but it was neither the coldest year nor that with the highest number of days with A5. The situation presented in the chart for June is similar (Figure 7b). The distribution of the dots for monthly values for June (b), July (c), and August (d) shows that the relation is smaller than for the entire summer season. As mentioned above and seen in Figure 7, there are many zero values on the monthly series for A5. In July and August, there is an absence of blue dots on the graphs because no one year covers the requirement for the temperature to be below the 10th percentile and, at the same time, the number of days with type A5 to be equal to or greater than the 90th percentile.

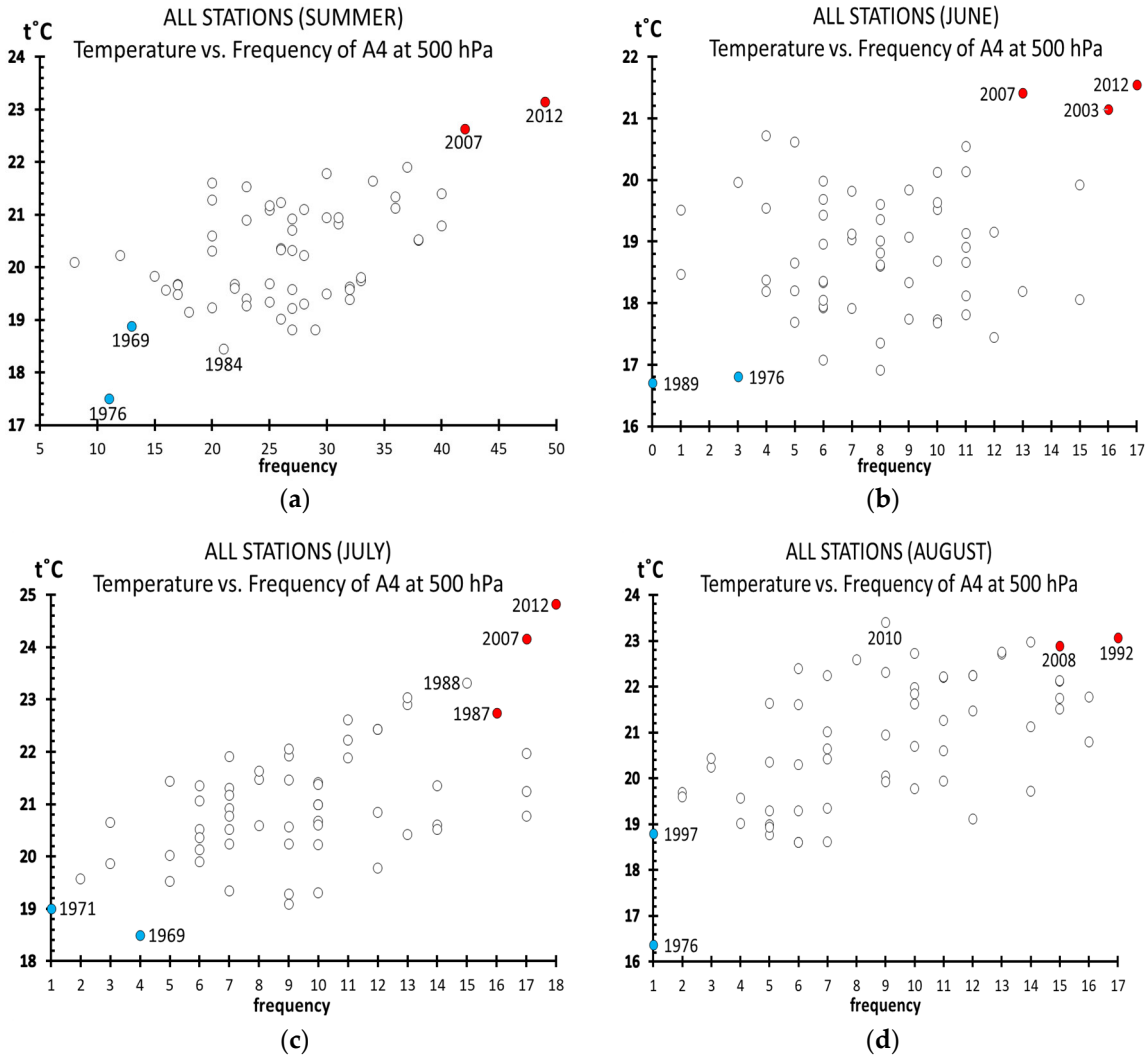

Figure 6. Relations between the average temperature (ordinate) for all studied meteorological stations and the number of days (frequency) with type A4 (abscissa) in the period (1961–2020) for (**a**) the summer season; (**b**) June; (**c**) July; and (**d**) August. The blue and red dots show the years in which both the temperature and the number of days with this circulation type fall, respectively, in the 10th and 90th percentiles.

The atmospheric circulation classification used in this research was made for the whole territory of Bulgaria and the neighbouring territories, as explained above in Section 2 Materials and Methods (Figure 2), so the number of days with the current circulation type is valid for the whole territory and, respectively, for all studied meteorological stations. Table 5 gives the results concerning type A4 individually for all examined stations on a seasonal and monthly basis. It is evident that the years within the 10th and 90th percentile thresholds for both parameters are similar across most regions of the relatively small territory of Bulgaria, although there are some regional differences. For example, July 1987 falls in the 90th percentile only in the western parts of the country, thus showing that the hot period in that month is more pronounced in western Bulgaria. August 1992 was one of the warmest for almost all of the country, except on the seaside and Sliven, less than 100 km west of it. Similar conclusions could be drawn for one of the coldest summer seasons in 1969 and the month of June 1976, which are not amongst the coldest in the eastern and southeastern parts of the country near the seaside. The temperature in July 1981 crossed the 10th percentile in the western, northwestern, and northeastern parts of Bulgaria, which is probably caused by cold fronts from the northwest in that month because these regions are

susceptible to stronger cold air intrusions in this way. However, such a regional implication could not be made for the cold August 1997 because the temperature falls within the 10th percentile threshold for stations in different regions. For all the other stations, the temperature was very close to this threshold, but it had not been reached. The situation was similar for the whole summer of 2008; the temperature achieved the 90th percentile only for three stations, but for the others, it was close to it but below the threshold. On a seasonal basis, the coldest and warmest years are almost the same, with some exceptions mentioned above. The gaps in Table 5 have no values, like August for Varna and Burgas and July for Varna, which means that there is no coincidence between the exceedance of the threshold for both temperature and the number of days with type A4. This is an interesting fact, but maybe logical, because of the lower coefficient of correlation between type A4 at the 500 hPa level in the middle troposphere and the surface temperature in the eastern direction near the seaside.

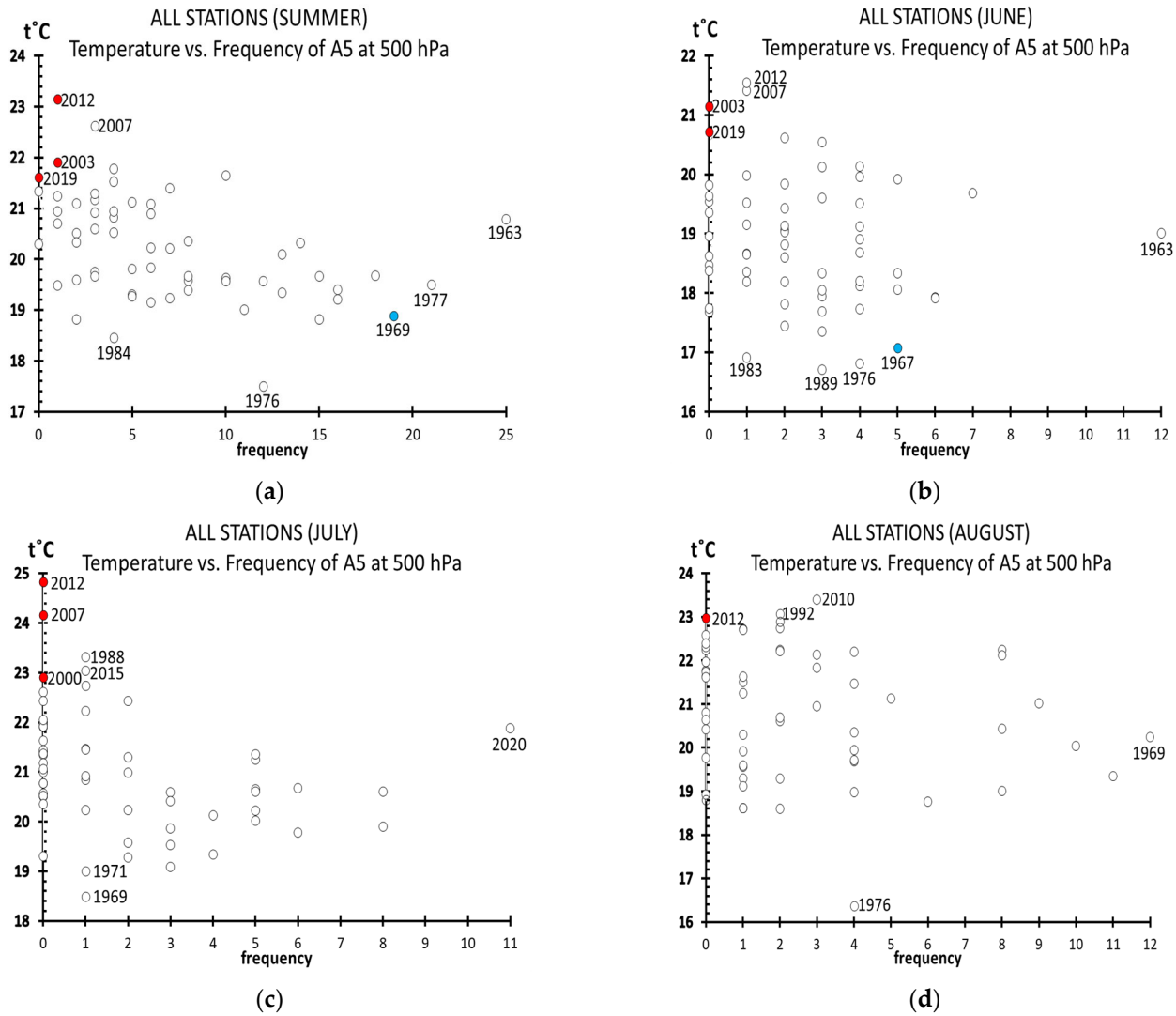

Figure 7. Relations between the average temperature (ordinate) for all studied meteorological stations and the number of days with type A5 (abscissa) in the period (1961–2020) for (**a**) the summer season; (**b**) June; (**c**) July; and (**d**) August. Blue and red dots show the years in which both the temperature and the number of days with this circulation type fall, respectively, in the 10th and 90th percentile.

Table 5. Years in which the number of days with type A4 and the temperature both exceed the 90th percentile threshold or are below the 10th percentile in the period (1961–2020) for the whole summer season and separately for June, July, and August. (t)—seasonal or monthly temperature; (n)—number of days with type A4.

Summer	VI	VII	VIII	Station	Summer	VI	VII	VIII
(t,n) $\leq$ p10	(t,n) $\leq$ p10	(t,n) $\leq$ p10	(t,n) $\leq$ p10	Type A4	(t,n) $\geq$ 90p	(t,n) $\geq$ 90p	(t,n) $\geq$ 90p	(t,n) $\geq$ 90p
1969, 1976	1976, 1989	1969, 1971	1976	Vidin	2007, 2012	2003, 2007, 2012	1987, 2007, 2012	1992
1969, 1976	1976, 1989	1969, 1971, 1981	1976	Pleven	2007, 2012	2003, 2007, 2012	1987, 2007, 2012	1992, 2000, 2008
1969, 1976	1976, 1989	1969, 1971, 1981	1976, 1997	Razgrad	2007, 2000, 2012	2003, 2007, 2012	2007, 2012	1992, 2008
1969, 1976	1976, 1989	1969, 1971, 1981	1976	Calarasi	2007, 2012	2003, 2007, 2012	2007, 2012	1992
1976	1989		1976, 1997	Varna	2007, 2012	2003, 2007, 2012	2007, 2012	
1976	1989	1969, 1971	1976	Burgas	2007, 2012	2003, 2007, 2012	2007, 2012	
1976	1976, 1989	1969, 1971	1976, 1997	Sliven	2007, 2012	2003, 2007, 2012	2007, 2012	2008
1976	1989	1969, 1971	1976, 1997	Kardzhali	2007, 2012	2003, 2007, 2012	2007, 2012	1992
1969, 1976	1976, 1989	1969, 1971	1976	Plovdiv	2007, 2012	2003, 2007, 2012	2007, 2012	1992
1969, 1976	1976, 1989	1969, 1971	1976, 1997	Sandanski	2007, 2008, 2012	2003, 2007, 2012	1987, 2007, 2012	1992, 2008
1969, 1976	1976, 1989	1969, 1971, 1981	1976, 1997	Kjustendil	2007, 2012	2003, 2007, 2012	1987, 2007, 2012	1963, 2000
1969, 1976	1976, 1989	1969, 1971	1976, 1997	Musala	2007, 2012	2003, 2007, 2012	1987, 2007, 2012	1992,2 008
1969, 1976	1976, 1989	1969, 1971, 1981	1976, 1997	Murgash	2007, 2012	2003, 2007, 2012	1987, 2007, 2012	1992, 2000
1969, 1976	1976, 1989	1969, 1971, 1981	1976	Sofia	2007, 2012	2003, 2007, 2012	1987, 2007, 2012	1992, 2000, 2008
1969, 1976	1976, 1989	1969, 1971	1976, 1997	Nis	2007, 2008, 2012	2003, 2007, 2012	1987, 2007, 2012	1992, 2000

Concerning type A5, Table 6 shows just the seasonal and not the monthly values of the number of days with type A5 and the temperature, falling in the 10th and 90th percentile thresholds, because the correlation coefficients every month are not statistically significant, except for July (Table 4). The correlation coefficient between A5 and the temperature is negative, so here the opposite conditions must be fulfilled: the temperature must be equal to and below the 10th percentile, and the number of days must be equal to and above the 90th percentile for extremely cold years and the opposite for extremely warm years. Like type A4, the years that fall within the thresholds are 1969 for the extremely cold summer seasons and 2012 for the extremely warm ones.

Table 6. Years in which the number of days with type A5 exceeds the 90th percentile threshold and the temperature is below the 10th percentile in the period (1961–2020) for the whole summer season for extremely cold years and the opposite for extremely warm years. (t)—seasonal temperature; (n)—number of days with type A5.

Summer	Station	Summer
t ≤ p10; n ≥ 90p	**Type A5**	**t ≥ 90p; n ≤ p10**
1968, 1969	Vidin	2003, 2012
1969	Pleven	2003, 2012
1969	Razgrad	2003, 2012
1969	Calarasi	2003, 2012, 2019
	Varna	2012, 2019
1974	Burgas	2003, 2012, 2019
	Sliven	2003, 2012
	Kardzhali	2003, 2012
1969	Plovdiv	1998, 2003, 2012
1969	Sandanski	2012
1969	Kjustendil	2012, 2015, 2019
1969, 1974	Musala	2012, 2019
1969	Murgash	2003, 2012, 2019
1969	Sofia	2003, 2012, 2019
1969	Nis	2003, 2012, 2019

3.4. Trends of A4 and A5 Anticyclonic Types at the 500 hPa Level in the Summer Seasons

The frequencies of types A4 and A5 during every summer season in the examined 60-year period are shown in Figure 8. The blue and red-coloured years in the figure represent the coldest and warmest summers. fulfilling the thresholds of the 10th and 90th percentiles for both seasonal temperature and the number of days of the current type. The applied Man–Kendall test and Sen's slope estimator on both rows show a statistically significant decrease in A5 (p-value/2.02 × 10^{-9}) and an increase in A4, but these are statistically insignificant (p-value/0.25).

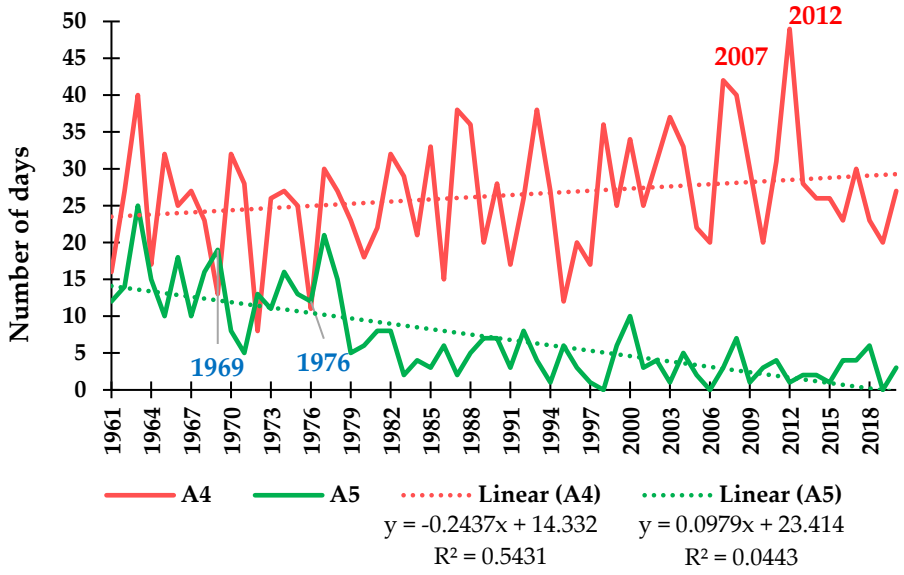

Figure 8. Number of days of types A4 and A5 at the 500 hPa level in summer seasons in the period (1961–2020).

The decrease in A5 is nearly 187% relative to its average value of 6.9 days per season, and the increase in A4 is 16% at an average value of 26.4 days for the summer season. At the beginning of the period, the frequencies of both types are close to each other and even almost equal, but gradually the presence of A4 increases, while that of A5 does not. Type A4 had its record frequency in 2012 of 49 days, which is more than half of the whole summer season, consisting of 92 days. The average summer seasonal temperature for all the studied meteorological stations in the period 1961–2020 is illustrated in Figure 9. The highest summer temperature was also reached in 2012, followed by 2007. The trend is positive and statistically significant.

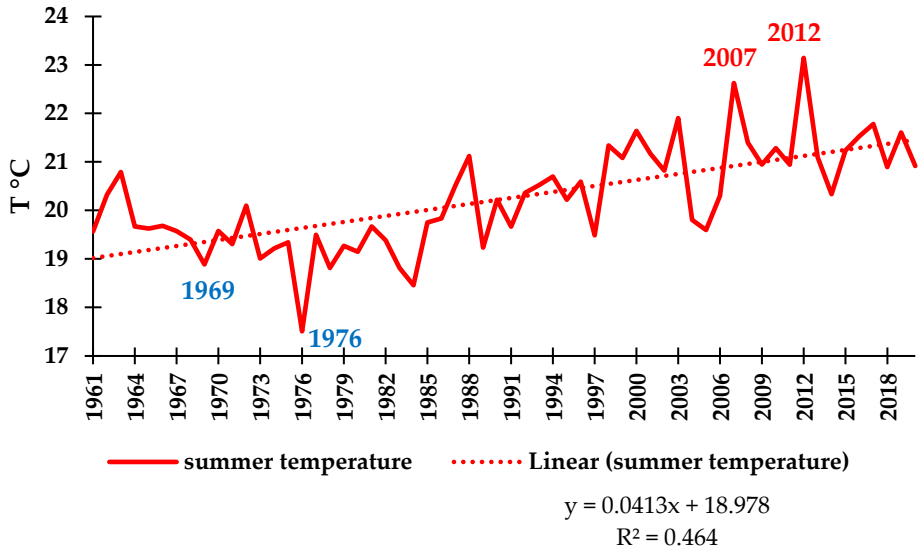

Figure 9. Average summer temperature for all examined stations (1961–2020).

Taking into account the positive and statistically significant correlation with the temperature, its positive trend and one of the highest frequencies amongst all circulation types, we can conclude that the increased frequencies of A4 reinforce the warming in the central parts of the Balkan peninsula and especially in Bulgaria during the summer season. The opposite is valid for type A5 because, despite its lower frequency, its cooling effect has been limited in the last decades, due to its negative tendency.

4. Conclusions

Comparing the last two 30-year climatological periods (1961–1990) and (1991–2020), an undoubtedly rapid decrease in extremely cold summer seasons and summer months in the last 30 years has occurred, and at the same time, a rapid increase in extremely warm summer seasons and months was found, according to the accepted thresholds of the 10th and 90th percentiles. The highest number of extremely warm seasons was established during 1991–2020 along the seaside, and, at the same time, extremely cold seasons were not registered there at all. The reason for this fact is the rise in the frequency of type A4 on one side and the increase in the sea surface water temperature on the other. The correlation between circulation types and the temperature shows the warming effect at least on the middle part of the Balkans of Azores anticyclone at the 500 hPa baric level in the middle troposphere (type A4). August has the highest and most statistically significant correlation coefficient between type A4 and the temperature of all summer months. In most cases, anticyclones or ridges with a centre south and southeast of Bulgaria (type A5) have a cooling effect, although the direction of the air masses during the presence of this type is most often from the southwest. This fact is probably related to the neighbouring high troughs or cyclones situated west of the anticyclone over the middle Mediterranean, which means relatively colder air there. Such a kind of circulation at 500 hPa could be a reason for cyclogenesis in the lower levels and eventually cloudiness, possible precipitations, and,

therefore, relatively lower temperatures, especially in the summer. The increasing trend in the frequencies of warming type A4 and the decrease in cooling type A5 prove that the change in the atmospheric circulation in the middle troposphere, concerning at least anticyclones, is one of the major reasons for the warming summers over the central Balkans in recent decades.

Author Contributions: Conceptualization, V.P., N.N. and S.M.; methodology, V.P., S.M. and M.G.; software, V.P.; validation, S.M.; formal analysis, V.P., N.N. and S.M.; investigation, V.P.; resources, V.P. and S.M.; data curation, V.P.; writing—original draft preparation, V.P.; writing—review and editing, V.P., N.N., S.M. and M.G.; visualization, V.P. All authors have read and agreed to the published version of the manuscript.

Funding: This research was funded by the National Science Programme "Environmental Protection and Reduction of Risks of Adverse Events and Natural Disasters", approved by the Resolution of the Council of Ministers № 577/17.08.2018 and supported by the Ministry of Education and Science (MES) of Bulgaria (Agreement № Д01-271/09.12.2022) and by the Programme for Funding Multilateral Scientific and Technological Cooperation Projects in the Danube Region (grant numbers DS-FR-22-0017, the Slovak Research and Development Agency, and KP-Danube-1/18.07.2023, the Ministry of Education and Science). It was also supported by the National Science Fund of Bulgaria, Contract КП-06-Н34/1 (KP-06-N34/1) "Natural and anthropogenic factors of climate change—analyzes of global and local periodical components and long-term forecasts".

Institutional Review Board Statement: Not applicable.

Informed Consent Statement: Not applicable.

Data Availability Statement: The data presented in this study are available on request from the corresponding author. The data are not publicly available due to privacy.

Acknowledgments: We would like to thank the anonymous reviewers for their time and comments. Support for the Twentieth-Century Reanalysis Project version 2c dataset was provided by the U.S. Department of Energy, the Office of Science Biological and Environmental Research (BER), and by the National Oceanic and Atmospheric Administration Climate Programme Office. The synoptic images of the anticyclonic types were generated with the help of NOAA-CIRES 20th-Century Reanalysis (V2c) data provided by the NOAA PSL, Boulder, Colorado, USA, from their website at https://psl.noaa.gov (accessed on 15 May 2024).

Conflicts of Interest: The authors declare no conflicts of interest.

References

1. Sfică, L.; Croitoru, A.E.; Iordache, I.; Ciupertea, A.F. Synoptic conditions generating heat waves and warm spells in Romania. *Atmosphere* **2017**, *8*, 50. [CrossRef]
2. Tomczyk, A.M.; Piotrowski, P.; Bednorz, E. Warm spells in Northern Europe in relation to atmospheric circulation. *Theor. Appl. Climatol.* **2017**, *128*, 623–634. [CrossRef]
3. Katsoulis, B.D.; Hatzianastassiou, N. Analysis of hot spell characteristics in the Greek region. *Clim. Res.* **2005**, *28*, 229–241. [CrossRef]
4. Colacino, M.; Conte, M. Heat waves in the central Mediterranean. A synoptic climatology. *Il Nuovo C. C* **1995**, *18*, 295–304.
5. Rusticucci, M.; Vargas, W. Synoptic situations related to spells of extreme temperatures over Argentina. *Meteorol. Appl.* **1995**, *2*, 291–300. [CrossRef]
6. Runyon, S.C.; Bosart, L.F. A Statistical analysis and synoptic climatology of heat waves over the United States. In Proceedings of the 21st Conference on Weather Analysis and Forecasting/17th Conference on Numerical Weather Prediction, Albany, NY, USA, 1 August 2005.
7. Grotjahn, R. *Western North American Extreme Heat, Associated Large Scale Synoptic-Dynamics, and Performance by a Climate Model*; Cambridge University Press: Cambridge, UK, 2016; pp. 198–209.
8. Min, K.H.; Chung, C.H.; Bae, J.H.; Cha, D.H. Synoptic characteristics of extreme heatwaves over the Korean Peninsula based on ERA Interim reanalysis data. *Int. J. Climatol.* **2020**, *40*, 3179–3195. [CrossRef]
9. Luo, M.; Lau, N.C. Synoptic characteristics, atmospheric controls, and long-term changes of heat waves over the Indochina Peninsula. *Clim. Dyn.* **2018**, *51*, 2707–2723. [CrossRef]
10. Wang, W.; Zhou, W.; Li, X.; Wang, X.; Wang, D. Synoptic-scale characteristics and atmospheric controls of summer heat waves in China. *Clim. Dyn.* **2016**, *46*, 2923–2941. [CrossRef]

11. Tringa, E.; Tolika, K.; Anagnostopoulou, C.; Kostopoulou, E. A Climatological and Synoptic Analysis of Winter Cold Spells over the Balkan Peninsula. *Atmosphere* **2022**, *13*, 1851. [CrossRef]
12. Pappas, C.; Hatzianastassiou, N.; Katsoulis, B.D. Analysis of cold spells in the Greek region. *Clim. Res.* **2004**, *27*, 211–223. [CrossRef]
13. Aalijahan, M.; Salahi, B.; Rahimi, Y.G.; Asl, M.F. A new approach in temporal-spatial reconstruction and synoptic analysis of cold waves in the northwest of Iran. *Theor. Appl. Climatol.* **2019**, *137*, 341–352. [CrossRef]
14. Anagnostopoulou, C.; Tolika, K.; Lazoglou, G.; Maheras, P. The exceptionally cold January of 2017 over the Balkan Peninsula: A climatological and synoptic analysis. *Atmosphere* **2017**, *8*, 252. [CrossRef]
15. Zschenderlein, P.; Wernli, H. The unusually long cold spell and the snowstorm Filomena in Spain in January 2021. *Nat. Hazards Earth Syst. Sci. Discuss.* **2022**, 1–21. [CrossRef]
16. Demirtaş, M. The anomalously cold January 2017 in the south-eastern Europe in a warming climate. *Int. J. Climatol.* **2022**, *42*, 6018–6026. [CrossRef]
17. Reale, M.; Lionello, P. Synoptic climatology of winter intense precipitation events along the Mediterranean coasts. *Nat. Hazards Earth Syst. Sci.* **2013**, *13*, 1707–1722. [CrossRef]
18. Warner, M.D.; Mass, C.F.; Salathé, E.P. Wintertime extreme precipitation events along the Pacific Northwest coast: Climatology and synoptic evolution. *Mon. Weather Rev.* **2012**, *140*, 2021–2043. [CrossRef]
19. Wu, Y.C.; Wang, S.Y.S.; Yu, Y.C.; Kung, C.Y.; Wang, A.H.; Los, S.A.; Huang, W.R. Climatology and change of extreme precipitation events in Taiwan based on weather types. *Int. J. Climatol.* **2019**, *39*, 5351–5366. [CrossRef]
20. Bluestein, H.B.; Parks, C.R. A synoptic and photographic climatology of low-precipitation severe thunderstorms in the southern plains. *Mon. Weather Rev.* **1983**, *111*, 2034–2046. [CrossRef]
21. Viale, M.; Nuñez, M.N. Climatology of winter orographic precipitation over the subtropical central Andes and associated synoptic and regional characteristics. *J. Hydrometeorol.* **2011**, *12*, 481–507. [CrossRef]
22. Quinting, J.F.; Catto, J.L.; Reeder, M.J. Synoptic climatology of hybrid cyclones in the Australian region. *Q. J. R. Meteorol. Soc.* **2019**, *145*, 288–302. [CrossRef]
23. Collins, M.J.; Kirk, J.P.; Pettit, J.; DeGaetano, A.T.; McCown, M.S.; Peterson, T.C.; Means, T.N.; Zhang, X. Annual floods in New England (USA) and Atlantic Canada: Synoptic climatology and generating mechanisms. *Phys. Geogr.* **2014**, *35*, 195–219. [CrossRef]
24. Gamble, D.W.; Meentemeyer, V.G. A synoptic climatology of extreme unseasonable floods in the southeastern United States, 1950–1990. *Phys. Geogr.* **1997**, *18*, 496–524. [CrossRef]
25. Kahana, R.; Ziv, B.; Enzel, Y.; Dayan, U. Synoptic climatology of major floods in the Negev Desert, Israel. *Int. J. Climatol. A J. R. Meteorol. Soc.* **2002**, *22*, 867–882. [CrossRef]
26. Lamb, H.H. British Isles Weather Types and a Register of Daily Sequence of Circulation Patterns, 1861–1971. In *Geophysical Memoirs*; HMSO: London, UK, 1972; Volume 116, 85p.
27. O'Hare, G.; Sweeney, J. Lamb's circulation types and British weather: An evaluation. *Geography* **1993**, *78*, 43–60.
28. Hess, P.; Brezowsky, H. *Katalog der Grosswetterlagen Europas. Ber. Dt. Wetterd. US-zone Nr.33, 1952. 39 S.*; neue erweiterte Auflage des wahrend des Krieges von. F. Baur, P. Hess und H. Nagel bearbeiteten und nicht veroffentlichten Kalenders der Groswetterlagen Europas vom 1. Januar 1881 bis 31. Dezember 1943. Hamburg 1944; Deutscher Wetterdienst: Hamburg, Germany, 1952.
29. Gerstengarbe, F.W.; Werner, P.C.; Rüge, U. *Katalog der Grosswetterlagen Europas (1881–1998) nach Paul Hess und Helmuth Brezowsky 1999*; Potsdam-Institut für Klimafolgenforschung: Potsdam, Germany, 1969.
30. Hess, P.; Brezowsky, H. Katalog der Groûwetterlagen Europas. 2. Neu bearbunderg Aufl. *Berichte Des Dtsch. Wetterdienstes Offenb.* **1969**, *113*, 52.
31. Maheras, P.; Patrikas, I.; Karacostas, T.; Anagnostopoulou, C. Automatic classification of circulation types in Greece: Methodology, description, frequency, variability and trend analysis. *Theor. Appl. Clim.* **2000**, *67*, 205–223. [CrossRef]
32. Maheras, P.; Tolika, K.; Anagnostopoulou, C.; Vafiadis, M.; Patrikas, I.; Flocas, H. On the relationships between circulation types and changes in rainfall variability in Greece. *Int. J. Clim.* **2004**, *24*, 1695–1712. [CrossRef]
33. Maheras, P.; Flocas, H.; Tolika, K.; Anagnostopoulou, C.; Vafiadis, M. Circulation types and extreme temperature changes in Greece. *Clim. Res.* **2006**, *30*, 161–174. [CrossRef]
34. Pophristov, V.; Peneva, E. Classification of circulation types over Bulgaria: Method description, frequency, variability and trend analysis. *Int. J. Adv. Res.* **2018**, *6*, 1289–1305. [CrossRef]
35. Malcheva, K.; Pophristov, V.; Marinova, T.; Trifonova, L. Complex approach for classification of winter severity in Bulgaria. In *AIP Conference Proceedings (Melville USA)*; AIP Publishing: College Park, MD, USA, 2019; Volume 2075.
36. Bocheva, L.; Pophristov, V. Seasonal analysis of large-scale heavy precipitation events in Bulgaria. In *AIP Conference Proceedings*; AIP Publishing: College Park, MD, USA, 2019; Volume 2075.
37. Skinner, W.R.; Flannigan, M.D.; Stocks, B.J.; Martell, D.L.; Wotton, B.M.; Todd, J.B.; Bosch, E.M. A 500 hPa synoptic wildland fire climatology for large Canadian forest fires, 1959–1996. *Theor. Appl. Climatol.* **2002**, *71*, 157–169. [CrossRef]
38. Skinner, W.R.; Stocks, B.J.; Martell, D.L.; Bonsal, B.; Shabbar, A. The association between circulation anomalies in the mid-troposphere and area burned by wildland fire in Canada. *Theor. Appl. Climatol.* **1999**, *63*, 89–105. [CrossRef]
39. Hayasaka, H.; Tanaka, H.L.; Bieniek, P.A. Synoptic-scale fire weather conditions in Alaska. *Polar Sci.* **2016**, *10*, 217–226. [CrossRef]

40. Amraoui, M.; Pereira, M.G.; DaCamara, C.C.; Calado, T.J. Atmospheric conditions associated with extreme fire activity in the Western Mediterranean region. *Sci. Total Environ.* **2015**, *524*, 32–39. [CrossRef] [PubMed]
41. Pereira, M.G.; Trigo, R.M.; da Camara, C.C.; Pereira, J.M.; Leite, S.M. Synoptic patterns associated with large summer forest fires in Portugal. *Agric. For. Meteorol.* **2005**, *129*, 11–25. [CrossRef]
42. Richardson, D.; Black, A.S.; Monselesan, D.P.; Risbey, J.S.; Squire, D.T.; Tozer, C.R.; Canadell, J.G. Increased extreme fire weather occurrence in southeast Australia and related atmospheric drivers. *Weather Clim. Extrem.* **2021**, *34*, 100397. [CrossRef]
43. Sun, Y.; Niu, T.; He, J.; Ma, Z.; Liu, P.; Xiao, D.; Yan, X. Classification of circulation patterns during the formation and dissipation of continuous pollution weather over the Sichuan Basin, China. *Atmos. Environ.* **2020**, *223*, 117244. [CrossRef]
44. Gao, D.; Xie, M.; Chen, X.; Wang, T.; Liu, J.; Xu, Q.; Ren, J. Systematic classification of circulation patterns and integrated analysis of their effects on different ozone pollution levels in the Yangtze River Delta Region, China. *Atmos. Environ.* **2020**, *242*, 117760. [CrossRef]
45. Zhou, C.; Wei, G.; Xiang, J.; Zhang, K.; Li, C.; Zhang, J. Effects of synoptic circulation patterns on air quality in Nanjing and its surrounding areas during 2013–2015. *Atmos. Pollut. Res.* **2018**, *9*, 723–734. [CrossRef]
46. He, J.; Gong, S.; Zhou, C.; Lu, S.; Wu, L.; Chen, Y.; Yin, C. Analyses of winter circulation types and their impacts on haze pollution in Beijing. *Atmos. Environ.* **2018**, *192*, 94–103. [CrossRef]
47. Gu, S.; Wu, S.; Yang, L.; Hu, Y.; Tian, B.; Yu, Y.; Zhang, B. Synoptic Weather Patterns and Atmospheric Circulation Types of PM2. 5 Pollution Periods in the Beijing-Tianjin-Hebei Region. *Atmosphere* **2023**, *14*, 942. [CrossRef]
48. Zheng, X.Y.; Fu, Y.F.; Yang, Y.J.; Liu, G.S. Impact of atmospheric circulations on aerosol distributions in autumn over eastern China: Observational evidence. *Atmos. Chem. Phys.* **2015**, *15*, 12115–12138. [CrossRef]
49. Ormanova, G.; Karaca, F.; Kononova, N. Analysis of the impacts of atmospheric circulation patterns on the regional air quality over the geographical center of the Eurasian continent. *Atmos. Res.* **2020**, *237*, 104858. [CrossRef]
50. Fotros, S.; Meshkatee, A.H.; Kamali, G.; Sedaghatkerdar, A. Exploring the most influential part of atmospheric circulation in the formation of severe air pollution episodes in the Greater Tehran. *Arab. J. Geosci.* **2018**, *11*, 1–18. [CrossRef]
51. Thomas, M.A.; Devasthale, A.; Nygård, T. Influence of springtime atmospheric circulation types on the distribution of air pollutants in the Arctic. *Atmos. Chem. Phys.* **2021**, *21*, 16593–16608. [CrossRef]
52. Valverde, V.; Pay, M.T.; Baldasano, J.M. Circulation-type classification derived on a climatic basis to study air quality dynamics over the Iberian Peninsula. *Int. J. Climatol.* **2015**, *35*, 2877–2897. [CrossRef]
53. Raziei, T.; Azizi, G.; Mohammadi, H.; Khoshakhlagh, F. 500 Hpa Wintertime Daily Circulation Types over Iran and the Middle East. *Phys. Geogr. Res. Q.* **2011**, *42*, 17–34.
54. Fraedrich, K.; Bantzer, C.; Burkhardt, U. Winter climate anomalies in Europe and their associated circulation at 500 hPa. *Clim. Dyn.* **1993**, *8*, 161–175. [CrossRef]
55. Weaver, S.M.; Guinan, P.E.; Semenova, I.G.; Aloysius, N.; Lupo, A.R.; Hunt, S. A Case Study of Drought during Summer 2022: A Large-Scale Analyzed Comparison of Dry and Moist Summers in the Midwest USA. *Atmosphere* **2023**, *14*, 1448. [CrossRef]
56. Wang, Y.; Sun, X. Features and Evolution of Autumn Weather Regimes in the Southeast China. *Atmosphere* **2022**, *13*, 1734. [CrossRef]
57. Sulikowska, A.; Wypych, A. Summer temperature extremes in Europe: How does the definition affect the results? *Theor. Appl. Climatol.* **2020**, *141*, 19–30. [CrossRef]
58. Stephenson, D.B.; Diaz, H.F.; Murnane, R.J. Definition, diagnosis, and origin of extreme weather and climate events. *Clim. Extrem. Soc.* **2008**, *340*, 11–23.
59. Field, C.B.; Barros, V.; Stocker, T.F.; Qin, D.; Dokken, D.J.; Ebi, K.L.; Mastrandrea, M.D.; Mach, K.J.; Plattner, G.-K.; Allen, S.K.; et al. (Eds.) *Managing the Risks of Extreme Events and Disasters to Advance Climate Change Adaptation*; Cambridge University Press: Cambridge, UK, 2012.
60. Data, C. Guidelines on analysis of extremes in a changing climate in support of informed decisions for adaptation. *World Meteorol. Organ.* **2009**, *1500*, 72.
61. Zhang, X.; Alexander, L.; Hegerl, G.C.; Jones, P.; Tank, A.K.; Peterson, T.C.; Zwiers, F.W. Indices for monitoring changes in extremes based on daily temperature and precipitation data. *Wiley Interdiscip. Rev. Clim. Chang.* **2011**, *2*, 851–870. [CrossRef]
62. Ustrnul, Z.; Wypych, A.; Kosowski, M. Extreme temperatures and precipitation in Poland—An evaluation attempt. *Meteorol. Z.* **2012**, *21*, 37–47. [CrossRef] [PubMed]
63. Alexander, L.V.; Zhang, X.; Peterson, T.C.; Caesar, J.; Gleason, B.; Klein Tank, A.M.G.; Haylock, M.; Collins, D.; Trewin, B.; Rahimzadeh, F.; et al. Global observed changes in daily climate extremes of temperature and precipitation. *J. Geophys. Res.* **2006**, *111*, 1–22. [CrossRef]
64. Moberg, A.; Jones, P.D.; Lister, D.; Walther, A.; Brunet, M.; Jacobeit, J.; Alexander, L.V.; Della-Marta, P.M.; Luterbacher, J.; Yiou, P.; et al. Indices for daily temperature and precipitation extremes in Europe analyzed for the period 1901–2000. *J. Geophys. Res.* **2006**, *111*, D22106. [CrossRef]
65. Fischer, E.M.; Schär, C. Consistent geographical patterns of changes in high-impact European heatwaves. *Nat. Geosci.* **2010**, *3*, 398–403. [CrossRef]
66. Tomczyk, A.M.; Półrolniczak, M.; Kolendowicz, L. Cold waves in Poznań (Poland) and thermal conditions in the city during selected cold waves. *Atmosphere* **2018**, *9*, 208. [CrossRef]

67. Sanderson, M.; Economou, T.; Salmon, K.; Jones, S. Historical trends and variability in heat waves in the United Kingdom. *Atmosphere* **2017**, *8*, 191. [CrossRef]
68. Lhotka, O.; Kyselý, J. Hot Central-European summer of 2013 in a long-term context. *Int. J. Clim.* **2015**, *35*, 4399–4407. [CrossRef]
69. Revich, B.; Shaposhnikov, D. Excess mortality during heat waves and cold spells in Moscow, Russia. *Occup. Environ. Med.* **2008**, *65*, 691–696. [CrossRef]
70. Topliysky, D. *The Climate of Bulgaria*; Foundation Amstels: Sofia, Bulgaria, 2006; 300p. (In Bulgarian)
71. Weiss, A.; Hays, C.J. Calculating daily mean air temperatures by different methods: Implications from a non-linear algorithm. *Agric. For. Meteorol.* **2005**, *128*, 57–65. [CrossRef]
72. Kolyvas, C.; Missiakoulis, S.; Gofa, F. Mean Daily Temperature Estimations and the Impact on Climatological Applications. *Environ. Sci. Proc.* **2023**, *26*, 131. [CrossRef]
73. Compo, G.P.; Whitaker, J.S.; Sardeshmukh, P.D.; Matsui, N.; Allan, R.J.; Yin, X.; Worley, S.J. The twentieth century reanalysis project. *Q. J. R. Meteorol. Soc.* **2011**, *137*, 1–28. [CrossRef]
74. Saha, S.S.; Moorthi, H.; Pan, X.; Wu, J.; Wang, S.; Nadiga, P.; Tripp, R.; Kistler, J.; Woollen, D.; Behringer, H.; et al. The NCEP Climate Forecast System Reanalysis. *Bull. Amer. Meteor. Soc.* **2010**, *91*, 1015–1058. [CrossRef]
75. Kalnay, E.M.; Kanamitsu, R.; Kistler, W.; Collins, D.; Deaven, L.; Gandin, M.; Iredell, S.; Saha, G.; White, J.; Woollen, Y.; et al. The NCEP/NCAR 40—Year Reanalysis Project. Bull. *Amer. Meteor. Soc.* **1996**, *77*, 437–471. [CrossRef]
76. Available online: https://wetter3.de/archiv_gfs_dt.html (accessed on 18 December 2023).
77. Kendall, M.G. Rank Correlation Methods. By Maurice, G.; Kendall, MA [Pp. Vii + 160. London: Charles Griffinand Co. Ltd., 42 Drury Lane, 1948. 18 S]. *J. Inst. Actuar* **1949**, *75*, 140–141.
78. Sen, P.K. Estimates of the regression coefficient based on Kendall's tau. *J. Am. Stat. Assoc.* **1968**, *63*, 1379–1389. [CrossRef]
79. Gocic, M.; Trajkovic, S. Analysis of changes in meteorological variables using Mann-Kendall and Sen's slope estimator statistical tests in Serbia. *Glob. Planet. Chang.* **2013**, *100*, 172–182. [CrossRef]
80. Malcheva, K.; Bocheva, L.; Chervenkov, H. Spatio-Temporal Variation of Extreme Heat Events in Southeastern Europe. *Atmosphere* **2022**, *13*, 1186. [CrossRef]
81. Zahradníček, P.; Brázdil, R.; Řehoř, J.; Lhotka, O.; Dobrovolný, P.; Štěpánek, P.; Trnka, M. Temperature extremes and circulation types in the Czech Republic, 1961–2020. *Int. J. Climatol.* **2020**, *42*, 4808–4829. [CrossRef]
82. Sfîcă, L.; Niță, A.; Iordache, I.; Ilie, N. Specific weather conditions on Romanian territory for Hess-Brezowsky westerly circulation type. In Proceedings of the 15th International Multidisciplinary Scientific Geo Conference SGEM 2015, Conference Proceedings, Albena, Bulgaria, 18–24 June 2015; Volume 4, pp. 1073–1080, ISBN 978-619-7105-38-4. [CrossRef]
83. Bartoszek, K. The main characteristics of atmospheric circulation over East-Central Europe from 1871 to 2010. *Meteorol. Atmos. Phys.* **2017**, *129*, 113–129. [CrossRef]

Disclaimer/Publisher's Note: The statements, opinions and data contained in all publications are solely those of the individual author(s) and contributor(s) and not of MDPI and/or the editor(s). MDPI and/or the editor(s) disclaim responsibility for any injury to people or property resulting from any ideas, methods, instructions or products referred to in the content.